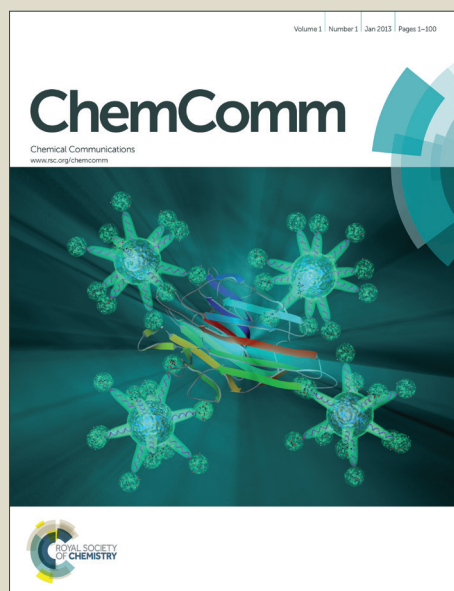


# ChemComm

Accepted Manuscript



This article can be cited before page numbers have been issued, to do this please use: M. Taneda, K. Shizu, H. Tanaka and C. Adachi, *Chem. Commun.*, 2015, DOI: 10.1039/C5CC00511F.



This is an *Accepted Manuscript*, which has been through the Royal Society of Chemistry peer review process and has been accepted for publication.

*Accepted Manuscripts* are published online shortly after acceptance, before technical editing, formatting and proof reading. Using this free service, authors can make their results available to the community, in citable form, before we publish the edited article. We will replace this *Accepted Manuscript* with the edited and formatted *Advance Article* as soon as it is available.

You can find more information about *Accepted Manuscripts* in the [Information for Authors](#).

Please note that technical editing may introduce minor changes to the text and/or graphics, which may alter content. The journal's standard [Terms & Conditions](#) and the [Ethical guidelines](#) still apply. In no event shall the Royal Society of Chemistry be held responsible for any errors or omissions in this *Accepted Manuscript* or any consequences arising from the use of any information it contains.

## COMMUNICATION

# High efficiency thermally activated delayed fluorescence based on 1,3,5-tris(4-(diphenylamino)phenyl)-2,4,6-tricyanobenzene

Cite this: DOI: 10.1039/x0xx00000x

Received 00th January 2012,  
Accepted 00th January 2012Masatsugu Taneda<sup>a</sup>, Katsuyuki Shizu<sup>a</sup>, Hiroyuki Tanaka<sup>a</sup>, and Chihaya Adachi<sup>a,b,c,\*</sup>

DOI: 10.1039/x0xx00000x

www.rsc.org/

A trigonal donor-acceptor molecule of 1,3,5-tris(4-(diphenylamino)phenyl)-2,4,6-tricyanobenzene (3DPA3CN) was synthesized to exhibit efficient thermally activated delayed fluorescence. By doping 3DPA3CN into a wide energy gap host, the film had a photoluminescence quantum efficiency of 100% with the reverse intersystem crossing efficiency of 100%. An OLED including the emitter exhibited very high external quantum efficiency ( $\eta_{\text{EQE}}$ ) of 21.4%.

Since Tang and VanSlyke reported the first, practical multilayered organic electroluminescent (EL) device in 1987,<sup>1</sup> organic light-emitting diodes (OLEDs) have been studied extensively. These studies have resulted in the commercialization of technology for flat-panel displays. One of the most critical issues in improving OLED performance is the enhancement of the external quantum efficiency. The external quantum efficiency,  $\eta_{\text{EQE}}$ , is given by  $\gamma \eta_{\text{ST}} \Phi_{\text{PL}} \Phi_{\text{out}}$ , where  $\gamma$  is charge carrier balance,  $\eta_{\text{ST}}$  is efficiency of exciton generation by carrier recombination,  $\Phi_{\text{PL}}$  is the photoluminescence (PL) quantum yield of the emissive layer, and  $\Phi_{\text{out}}$  is the light out-coupling efficiency. In particular, for the enhancement of emissive excitons, active management of the triplet excitons is the most important issue because singlets and triplets form in a ratio of 1:3.<sup>2</sup>

After the development of fluorescent materials, room temperature phosphorescent materials attracted much attention because both singlet and triplet excitons can be harvested for light emission as phosphorescence. Heavy metal complexes such as tris(phenylpyridine)iridium and their derivatives can convert the singlet excitons into triplet excitons through intersystem crossing (ISC) and the triplet excitons then decay radiatively. Although such phosphorescent metal complexes can harvest all excitons for light emission ( $\eta_{\text{ST}}$  and  $\Phi_{\text{PL}} = 1$ ), stable complexes with emission in the deep blue region of the spectrum are few. Additionally, the precious metals used in these complexes are expensive.

More recently, we proposed an alternative emissive mechanism instead of the conventional fluorescent and phosphorescent

materials. This is known as thermally activated delayed fluorescence (TADF) and is evident in third-generation luminescent materials. TADF can realize an ultimate electroluminescence (EL) efficiency through efficient upconversion from the lowest triplet excited state ( $T_1$ ) to the lowest singlet excited state ( $S_1$ ) through reverse intersystem crossing (RISC).<sup>3</sup> Our recent study showed that TADF strongly depends on the distribution and separation of the highest occupied molecular orbital (HOMO) and the lowest unoccupied molecular orbital (LUMO) in a single molecule. The preparation of a sufficiently small energy gap between  $S_1$  and  $T_1$  ( $\Delta E_{\text{ST}}$ ) enables efficient upconversion of triplet excitons from  $T_1$  to  $S_1$ , leading to nearly 100% singlet exciton formation ( $\eta_{\text{ST}} = 1$ ). We note that because the separation of the HOMO and the LUMO reduces the radiative transition probability, a small overlap of the HOMO and LUMO is necessary to ensure both a small  $\Delta E_{\text{ST}}$  and a large  $\Phi_{\text{PL}}$ . It is also important to prevent vibrational deactivation processes that compete with the radiative decay.

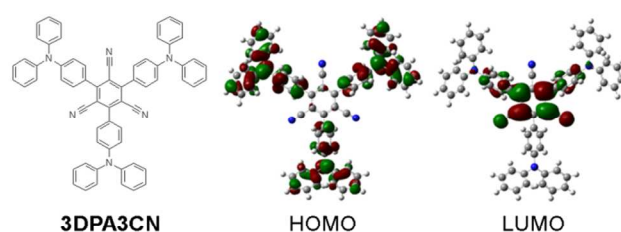


Fig. 1 The molecular structure and HOMO and LUMO of the 3DPA3CN calculated at the B3LYP/6-31G level of theory.

In this study, we designed the trigonal molecule 1,3,5-tris(4-(diphenylamino)phenyl)-2,4,6-tricyanobenzene (3DPA3CN). We expect that all six substitutions of the benzene ring with two different types of alternating substituents results in a decrease of vibrational deactivation because of the steric hindrance. Density functional theory (DFT) calculations<sup>4</sup> suggested that the introduction

## COMMUNICATION

of a phenylene linker bridging the diphenylamino groups and tricyanobenzene results in the separation of the HOMO and LUMO of **3DPA3CN** while keeping a moderate overlap between them (Fig. 1).

We expect that this planar structure would induce a horizontal molecular orientation. In our previous study, we showed that the van der Waals' interaction between a substrate surface and a molecule with a planar geometry induces a horizontal molecular orientation. Additionally, molecules with a donor-acceptor structure induce intermolecular interactions that can also influence the molecular orientation.<sup>5</sup> When the orientation of the transition dipole moment of the emitter molecules is parallel to a substrate, we can enhance the  $\Phi_{\text{out}}$  of an OLED significantly.<sup>6</sup> Although the  $\eta_{\text{EQE}}$  of OLEDs has been limited by the rather low outcoupling efficiency, a horizontal orientation of the emitters should enhance the  $\Phi_{\text{out}}$  by up to 45%.<sup>7</sup>

In this work, we synthesized **3DPA3CN** and investigated the fundamental photophysical and OLED characteristics. 1,3,5-tris(4-(diphenylamino)phenyl)-2,4,6-trifluorobenzene was synthesized as a precursor of **3DPA3CN** by Suzuki coupling of 1,3,5-tribromo-2,4,6-trifluorobenzene<sup>10</sup> and 2-(phenyl)-4,4,5,5-tetramethyl-1,3,2-dioxaborolane. The precursor was treated with KCN in DMSO to obtain **3DPA3CN**. The product was purified by sublimation (see further detail of the synthesis of **3DPA3CN** in the Supporting Information).

The ultraviolet-visible absorption and PL spectra of **3DPA3CN** in toluene are shown in Fig. 2. The broad absorption peak observed at around 420 nm can be assigned to the charge transfer (CT) transition from the diphenylamino groups to the tricyanobenzene moiety. Upon irradiation with ultraviolet light, **3DPA3CN** in degassed toluene emitted green light with a peak wavelength of 506 nm and  $\Phi_{\text{PL}}$  of 82%. When **3DPA3CN** (6 wt%) was co-deposited with bis(2-(diphenylphosphino)phenyl)ether oxide (DPEPO)<sup>11</sup> on a quartz substrate, the doped thin film had a green emission with a  $\Phi_{\text{PL}}$  of 100%, indicating complete suppression of non-radiative decay. The peak wavelength of the spectrum was 533 nm. The

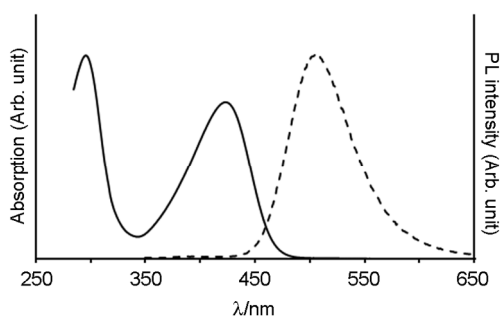


Fig. 2 The absorption (solid line) and emission (broken line) spectra of **3DPA3CN** in degassed toluene.

bathochromic shift is likely to be caused by the polarity of DPEPO.<sup>12</sup> Transient PL characteristics of the doped thin film (Fig. 3) showed both prompt and delayed emissions at 300 K. The prompt component had a transient decay time of 6.2 ns with an efficiency of 89.7% and the delayed component had a

decay time of 550  $\mu\text{s}$  and had an efficiency of 10.3%. The details of the transient decay characteristics are supplied in ESI. Because both spectra were nearly identical, the delayed component was attributed to TADF. From these PL characteristics, we estimated the numerical values of ISC rate ( $k_{\text{ISC}}$ ) =  $1.66 \times 10^7$ , RISC rate ( $k_{\text{RISC}}$ ) =  $2.03 \times 10^3$ , prompt fluorescence rate ( $k_{\text{p}}$ ) =  $1.61 \times 10^8$ , TADF rate ( $k_{\text{d}}$ ) =  $1.83 \times 10^3$ , and nonradiative decay rate ( $k_{\text{nr}}$ ) <  $10^5$ .

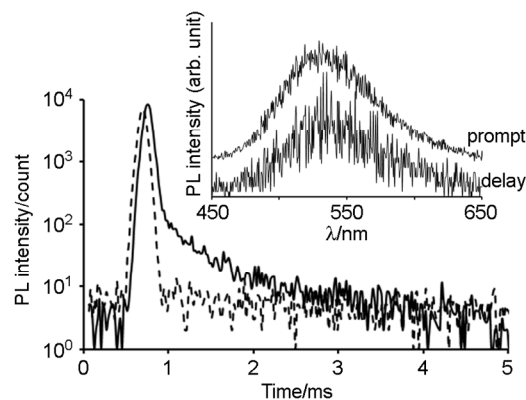
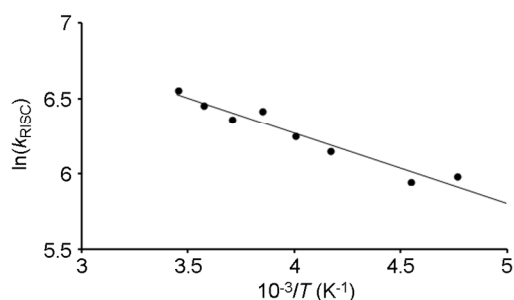


Fig. 3 The transient PL decay profile of a 6wt% **3DPA3CN**:DPEPO film measured at 300 K (solid line) and 100 K (broken line). The inset shows the PL spectra of the co-deposited film.

To evaluate  $\Delta E_{\text{ST}}$  quantitatively, the temperature dependence of RISC was measured. An Arrhenius plot was used to determine the activation energy of the RISC. We note that it was rather difficult to estimate the gap from the difference of fluorescence and phosphorescence spectra, since **3DPA3CN** showed no clear phosphorescence even at low temperature. We note that the activation energy would be slightly higher than the  $\Delta E_{\text{ST}}$ . The rate constant of the RISC ( $k_{\text{RISC}}$ ) can be estimated from experimentally determined rate constants and the  $\Phi_{\text{PL}}$  values of the prompt and delayed components at each temperature using<sup>13</sup>

$$k_{\text{RISC}} = \frac{k_{\text{p}} k_{\text{d}} \Phi_{\text{d}}}{k_{\text{ISC}} \Phi_{\text{p}}} \quad \text{Eq. (1)}$$

where  $k_{\text{p}}$  and  $k_{\text{d}}$  are the rate constants of the prompt and delayed fluorescence components, respectively,  $k_{\text{ISC}}$  is the rate constant of the transition of excitons from the  $T_1$  to the  $S_1$  state, and  $\Phi_{\text{p}}$  and  $\Phi_{\text{d}}$  are the PL quantum yields of the prompt and delayed components, respectively. Figure 4 shows  $k_{\text{RISC}}$  calculated using Equation (1) plotted against  $1/T$  for  $T = 200\text{--}300$  K. It was assumed that  $k_{\text{ISC}}$  was independent of temperature. The value of  $\Delta E_{\text{ST}}$  from the Arrhenius plot was 103 meV. Although the value of  $\Delta E_{\text{ST}}$  is not small,  $\Phi_{\text{PL}}$  of the **3DPA3CN** doped into DPEPO film was 100%, indicating that the trigonal structure of **3DPA3CN** suppresses nonradiative vibrational losses. We note that an mCP host also provided 100% PL quantum efficiency.



**Fig. 4** An Arrhenius plot of  $k_{\text{RISC}}$  where  $k_{\text{RISC}}$  was set to  $4 \times 10^{-7} \text{ s}^{-1}$ . The straight line fit (least-squares regression) was used to determine the activation energy. The evaluated  $\Delta E_{\text{ST}}$  was 103 meV.

To investigate the molecular orientation in thin films, the optical anisotropy was measured using variable angle spectroscopic ellipsometry (VASE).<sup>8,9</sup> If the molecular orientation is anisotropic, the optical properties parallel and perpendicular to the substrate will be different, leading to large differences in the refractive indices and extinction coefficients ( $k$ ) in the parallel (ordinary) and perpendicular (extraordinary) directions. Figure 5 shows the anisotropy of the extinction coefficients obtained using an analysis of the ellipsometric parameters from 245 to 1000 nm at seven different incident angles. To determine the molecular orientation, an orientation order parameter  $S$ <sup>9,14</sup> was calculated using

$$S = \frac{1}{4} - \frac{3}{4} \langle \cos^2 \left( \frac{\pi}{2} - \theta \right) \rangle = \frac{k_e - k_o}{k_e + 2k_o} \quad \text{Eq. (2)}$$

where  $\langle \dots \rangle$  is the ensemble average,  $\theta$  is the angle between the molecular  $\pi$ -plane and the direction perpendicular to the substrate surface, and  $k_o$  and  $k_e$  are the ordinary and extraordinary extinction coefficients at the peak wavelength.  $S = -0.5$  if the molecules are completely parallel to the surface and  $S = 0$  if they are randomly oriented. The ellipsometric analysis showed that **3DPA3CN** was oriented horizontally in the amorphous films and the average angle between the molecules and the substrate was  $29.5^\circ$  with the numerical values of  $k_e = 0.1304$  and  $k_o = 0.4710$  at the wavelength of 432 nm (Fig. 5a). The orientation of the guest materials doped

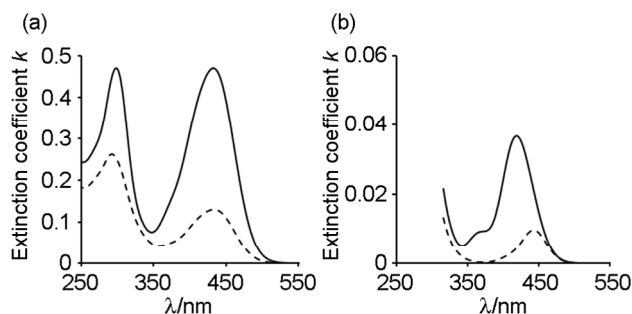


**Fig. 5** Extinction coefficients ( $k$ ) of (a) a neat **3DPA3CN** film and (b) a 6wt% **3DPA3CN**-doped DPEPO film in parallel (ordinary, solid line) and perpendicular (extraordinary, broken line) directions.  $k$  was obtained from the analysis of the ellipsometric parameters measured from 245 to 1000 nm or from 315 to 1000 nm at seven different incident angles.

with a host material with a low concentration cannot be determined because there is not sufficient detection sensitivity, and therefore ellipsometry is usually unsuitable. However, in the case of the 6wt%-**3DPA3CN**:DPEPO-doped film, the strong absorption band of **3DPA3CN** observed at around 420 nm was completely isolated from the absorption spectrum of DPEPO. This absorption band was used to detect the orientation of **3DPA3CN** using ellipsometry. As shown in Fig. 5b, **3DPA3CN** had a tendency to orient towards the horizontal in the DPEPO host layer. The average angle between the molecules and the substrate was confirmed to be  $30.8^\circ$  with the numerical values of  $k_e = 0.0106$  and  $k_o = 0.0350$  at the wavelength of 432 nm.

To confirm that high  $\Phi_{\text{PL}}$ , a small  $\Delta E_{\text{ST}}$  and a slight horizontal orientation of **3DPA3CN** would lead to a high  $\eta_{\text{EQE}}$ , we prepared an OLED with the structure of indium tin oxide (ITO)-coated glass/ $N,N'$ -di-[(1-naphthalenyl)- $N,N'$ -diphenyl]-(1,1'-biphenyl)-4,4'-diamine ( $\alpha$ -NPD)/ 3,3'-bis( $N$ -carbazole)-1,1'-biphenyl (mCBP)/ **3DPA3CN** (6 wt%) in DPEPO/1,3,5-tris(1-phenyl-1H-benzimidazol-2-yl) benzene (TPBi)/ LiF/ Al. In this architecture,  $\alpha$ -NPD is the hole transport layer, mCBP is the electron blocking layer, **3DPA3CN** in DPEPO is the emissive layer, TPBi is the electron transport layer, LiF is the electron injection layer, and Al is the cathode. As shown in Fig. 6, a maximum  $\eta_{\text{EQE}}$  of  $21.4 \pm 3\%$  at the current density  $J = 0.001 \text{ mA/cm}^2$  was obtained. We believe that the horizontal orientation of **3DPA3CN** in an emissive layer would contribute to enhance the  $\Phi_{\text{out}}$ .

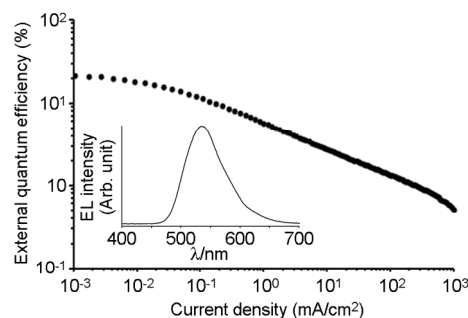


**Fig. 6** The dependence of the external electroluminescence quantum efficiency on the current density. The inset shows the EL spectrum.

In conclusion, we showed that **3DPA3CN** has excellent photophysical characteristics of a small  $\Delta E_{\text{ST}}$  of 103 meV and a high  $\Phi_{\text{PL}}$  of 100% in a 6wt%-**3DPA3CN**-doped DPEPO film. The preferential molecular orientation in both neat and doped films resulted in a fairly high  $\eta_{\text{EQE}}$  of 21.4%. We believe that further optimization of the device parameters will improve the  $\eta_{\text{EQE}}$ .

This research was supported by the Japan Society for the Promotion of Science (JSPS) through the ‘‘Funding Program for World-Leading Innovative R&D on Science and Technology (FIRST Program)’’, initiated by the Council for Science and Technology Policy (CSTP).

## Notes and references

## COMMUNICATION

<sup>a</sup> Center for Organic Photonics and Electronics Research (OPERA), Kyushu University, 744 Motoooka, Nishi, Fukuoka 819-0395, Japan. E-mail: adachi@cstf.kyushu-u.ac.jp

<sup>b</sup> JST, ERATO, Adachi Molecular Exciton Engineering Project, c/o OPERA, Kyushu University, 744 Motoooka, Nishi, Fukuoka 819-0395, Japan

<sup>c</sup> International Institute for Carbon Neutral Energy Research (WPI-I2CNER), Kyushu University, 744 Motoooka, Nishi, Fukuoka 819-0395, Japan

† Electronic Supplementary Information (ESI) available: Experimental and synthesis details, additional photophysical data, and supplementary figures and tables. See DOI: 10.1039/c000000x/

1 C. W. Tang, S. A. VanSlyke, Appl. Phys. Lett., 1987, **51**, 913-915.

2 a) M. A. Baldo, D. F. O'Brien, M. E. Thompson, S. R. Forrest, Phys. Rev. B: Condens. Matter Mater. Phys., 1999, **60**, 14422-14428; b) M. Segal, M. A. Baldo, R. J. Holmes, S. R. Forrest, Z. G. Soos, Phys. Rev. B: Condens. Matter Mater. Phys., 2003, **68**, 075211; c) B. H. Wallikewitz, D. Kabra, S. Gelinas, R. H. Friend, Phys. Rev. B: Condens. Matter Mater. Phys., 2012, **85**, 045209; d) T. Tsutsui, MRS Bull., 1997, **22**, 39.

3 a) A. Endo, M. Ogasawara, A. Takahashi, D. Yokoyama, Y. Kato, C. Adachi, Adv. Mater., 2009, **21**, 4802-4804; b) A. Endo, K. Sato, K. Yoshimura, T. Kai, A. Kawada, H. Miyazaki, C. Adachi, Appl. Phys. Lett., 2011, **98**, 083302; c) T. Nakagawa, S.-Y. Ku, K.-T. Wong, C. Adachi, Chem. Commun., 2012, **48**, 9580-9582; d) H. Tanaka, K. Shizu, H. Miyazaki, C. Adachi, Chem. Commun., 2012, **48**, 11392-11394; e) H. Uoyama, K. Goushi, K. Shizu, H. Nomura, C. Adachi, Nature, 2012, **492**, 234-240; f) H. Tanaka, K. Shizu, H. Nakanotani, C. Adachi, Chem. Mater., 2013, **25**, 3766-3771.

4 M. J. Frisch et al., GAUSSIAN 09, Revision B.01, Gaussian, Inc., Wallingford, CT, 2009.

5 M. Taneda, C. Adachi, Appl. Phys. Exp., submitting.

6 a) V. Bulovic, V. B. Khalfin, G. Gu, P. E. Burrows, D. Z. Garbuzov, S. R. Forrest, Phys. Rev. B 1998, **58**, 3730-3740; S. Nowy, B. C. Krummacker, J. Frischeisen, N. A. Reinke, W. Brütting, J. Appl. Phys., 2008, **104**, 123109.

7 J. Frischeisen, D. Yokoyama, A. Endo, C. Adachi, W. Brütting, Org. Electron., 2011, **12**, 809-817.

8 a) H.-W. Lin, C.-L. Lin, H.-H. Chang, Y.-T. Lin, C.-C. Wu, R.-T. Chen, Y.-Y. Chen, K.-T. Wong, J. Appl. Phys., 2004, **95**, 881-886; b) H. Fujiwara, Spectroscopic Ellipsometry: Principles and Applications, Wiley, New York, 2007; c) D. Yokoyama, A. Sakaguchi, M. Suzuki, C. Adachi, Appl. Phys. Lett., 2008, **93**, 173302.

9 D. Yokoyama, A. Sakaguchi, M. Suzuki, C. Adachi, Org. Electron., 2009, **10**, 127-137.

10 A. M. Kenwright, G. Sandford, A. J. Tadeusiak, D. S. Yufit, J. A.K. Howard, P. Kilickiran, G. Nelles, Tetrahedron, 2010, **66**, 9819-9827.

11 Q. Zhang, T. Komino, S. Huang, S. Matsunami, K. Goushi, and C. Adachi, Adv. Funct. Mater., 2012, **22**, 2327-2336.

12 R. Ishimatsu, S. Matsunami, K. Shizu, K. Shizu, C. Adachi, K. Nakano, T. Imato, J. Phys. Chem. A, 2013, **117**, 5607-5612.

13 K. Goushi, K. Yoshida, K. Sato, C. Adachi, Nature Photon., 2012, **6**, 253-258.

14 a) J. Y. Kim, D. Yokoyama, C. Adachi, J. Phys. Chem. C, 2012, **116**, 8699-8706; b) I. M. Ward, Structure and Properties of Oriented Polymers, Applied Science Publishers, London, 1975.